RHENIUM TRICARBONYL COMPLEX FEATURING AMINE MOIETIES AS MOLECULAR CATALYSTS FOR ELECTROCATALYTIC CO_2 REDUCTION

A Thesis

by

SOOMIN PARK

Submitted to the Office of Graduate and Professional Studies of
Texas A&M University
in partial fulfillment of the requirements for the degree of

MASTER OF SCIENCE

Chair of Committee,	Michael Nippe
Committee Members,	Marcetta Y. Darensbourg
	David C. Powers
	Haiyan Wang
Head of Department,	Simon North

May 2017

Major Subject: Chemistry

ABSTRACT

Molecular catalysts for the electrochemical reduction of CO_2 are being investigated for the potential utilization of CO_2 as a viable C1 feedstock for the chemical industry and energy economy. Various CO_2 reduction products can be generated such as CO, CH_3OH, and CH_4. Among the several multi-electron reduction products, this study focuses on the proton-coupled, two-electron reduction of CO_2 to generate selectively CO (and H_2O as the byproduct).

Several examples of selective CO_2 reduction electrocatalysts, such as $Ni(cyclam)^{2+}$, cobalt macrocyclic compounds based on azacalix[4](2,6)pyridines, and FeTDHPP (TDHPP = tetrakis(2',6'-dihydroxylphenyl)porphyrin), feature protic N-H or O-H groups in the vicinity of the reactive metal ion. Hydrogen-bonding like interactions between N-H groups and reduced CO_2 intermediates are proposed to stabilize transition states in $Ni(cyclam)^{2+}$ and cobalt macrocyclic compound, and the O-H groups in FeTDHPP are found to increase catalytic activity by acting as local proton sources.

Inspired by these reports, this study examines the effects of the interactions from the secondary coordination sphere of well-studied Lehn-type catalyst systems for CO_2 reduction. Lehn-type pre-catalysts feature $Re(CO)_3X$ (X = Cl, Br, and py) moieties coordinated to bipyridine or phenanthroline chelators and have been previously shown to be highly selective for CO_2 reduction.

ACKNOWLEDGEMENTS

I would like to thank my advisor, Dr. Michael Nippe, for all his guidance throughout the course of this research. In October 2015, I joined the Nippe group via "democratic decision-making" (I was so impressed), and now I am about to leave the group with this thesis. I have huge room for improvement to become an independent researcher; however, I still think that I am better than I used to be. With his hands-on style, I was able to learn more than ever before. Other than the research, I have been struggling with various hurdles, which sometimes extremely frustrated and discouraged me. Whenever I faced these difficulties, Dr. Nippe led me to see the bright side. Without your help and encouragement, I could not have made it this far. I truly appreciate all your support during my graduate study.

I also appreciate my committee members, Dr. Marcetta. Y. Darensbourg, Dr. David Powers, and Dr. Haiyan Wang for their guidance and supports. I first met Dr. M. Y. Darensbourg at her lecture in my first semester, and ever since, she has been a great mentor to my academic career. Every time I spoke with her about my difficulties, she motivated and encouraged me with kind words and smiles. Thank you always.

As Dr. Powers' office is only across mine, he found me locked out of the office several times. Every day, he greeted me while walking in the hallway. One day, when we had a conversation about my proposal, I made an awkward English mistake. I said, "Don't make me hurt you," but what I really meant was, "Don't hurt me". I do not know why you laughed out loud at that moment. You know that I did not mean it that way!

Dr. Wang, I appreciate all your help even though you are not on the campus. With your kindness, I have come this far to present my final defense. Thank you.

I cannot forget to mention Dr. Oleg Ozerov. When I was experiencing a personal crisis, he was there for me. With your advice, I overcame my hardship. At that moment, I relied on you more than my parents back home. I truly appreciate your support.

Thanks also go to my group members, Siyoung, Courtney, Corey, Trevor, and the Nippe group alumni, Dr. Davinder and Marcos (Or Carlos). My graduate life has been more dynamic than expected because of your presence. We have been through hard and good times together. I am very grateful that I have a group of people who I could share the feelings with and who understand me well.

I would like to thank all my friends in College Station, the department faculty and staff for making my time at Texas A&M University a great experience. I would like to thank Sandy for her encouragement and her help during my graduate studies.

Lastly, all my thanks go to my families and friends back home. All my old friends, thank you all for being a part of my life for several years, some even more than a decade. Even though I could not see you frequently, you all are still great supporters. I miss you all so much.

My family… Without your care, support, encouragement, calls, texts, and food packages, I could not have made it this far. Dad, you have understood me better through my difficulties since you have been through something similar. Now I know how hard it was for you. I do not know what my next step is, but I believe that your support will help me with my next decisions. Mom, I appreciate all your support. I am lucky to be your

daughter. Thank you for listening to all my stories from Texas, mostly difficulties and complaints. I felt a little relieved when we talked on the phone. My sister and brother, Sunmin and Yongsung, I am always here for you and will support you. I love you all.

Dewey, my love, you are the greatest thing that happened in my life. My time in Texas would have been very different without you. I cannot imagine how dark my time in Texas would be if you were not there. From the day we first met, you were always next to me, supporting me, and the most importantly feeding me. You are the only person who I rely on, and love (other than my family). My life has changed since I met you. You always make me smile every day. Thank you for being a part of my life. You have encouraged me to go forward and finally, finish my work. Thank you, my love.

CONTRIBUTORS AND FUNDING SOURCES

Contributors

This work was supervised by a thesis committee consisting of Professor Michael Nippe (chair), Professor Marcetta Y. Darensbourg and David C. Powers of the Department of Chemistry and Professor Haiyan Wang of the Department of Electrical and Computer Engineering.

All work for the thesis was completed by the student, under the advisement of Professor Michael Nippe of the Department of Chemistry.

Funding Sources

This work was made possible by New Faculty Start-up for Michael Nippe under Grant Number 02-216760-00220.

TABLE OF CONTENTS

Page

LIST OF FIGURES

Page

LIST OF TABLES

CHAPTER I

INTRODUCTION OF MOLECULAR CATALYSIS FOR CO_2 REDUCTION

I.1 The Significance of CO_2 Reduction on Society

Global warming has been one of the problems that the world faces for several decades. Greenhouse gases, including CO_2, methane, and fluorinated gases, cause the global warming by absorbing Infrared radiation from the sun and trapping it in globe atmosphere. According to a report from the U.S. Energy Information Administration, 81.5% of greenhouse gases in the US in 2009 come from energy-related CO_2 emission (Figure 1.1). In order to reduce the levels of CO_2 in the atmosphere, many researchers have been studying new approaches to use CO_2 as a C1 feedstock for the chemical industry as well as to generate fuels from CO_2 in sustainable ways by coupling its energetically uphill conversion to alternative energy sources. Utilizing electricity from a solar cell for CO_2 conversion into solar fuels is one method to store solar energy in chemical bonds. By capturing CO_2 from the atmosphere and generating chemicals from CO_2 using solar energy sources, a carbon neutral energy circle could be achieved.

I.2 CO_2 Reduction in Thermodynamic Perspective

CO_2 is a thermodynamically stable molecule, and thus it is a final combustion product of elemental carbon and hydrocarbons. Energy is necessary to convert a stable CO_2 molecule to value-added C1 chemicals. The minimum energy requirement for elec-

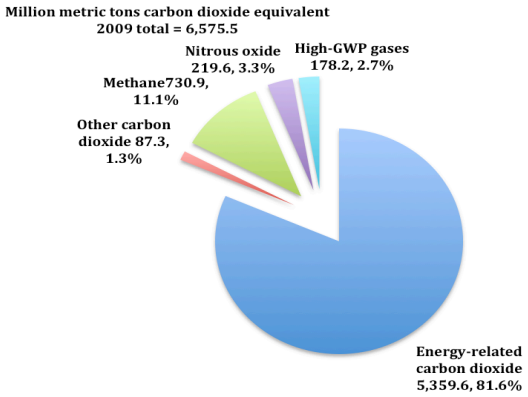

Figure 1.1 U.S. greenhouse gas emissions by gas. Adapted from Conti, J., *Emissions of Greenhouse Gases in the United States 2009*, 2011, pp 1-8.

trochemical reductions of CO_2 molecule to various products can be quantified as electrode potentials, and these are shown in Eqs 1.1-1.6. The reactions are at pH 7, and the potentials are vs NHE (Normal Hydrogen Electrode).[1]

$$CO_2\,(aq) + e^- \rightarrow CO_2^{\cdot -}\,(aq) \qquad E^{\circ\prime} = -1.90\ V \qquad \text{Eq 1.1}$$

$$CO_2\,(g) + 2H^+ + 2e^- \rightarrow CO\,(g) + H_2O \qquad E^{\circ\prime} = -0.52\ V \qquad \text{Eq 1.2}$$

$$CO_2\,(g) + H^+ + 2e^- \rightarrow HCO_2^-\,(aq) \qquad E^{\circ\prime} = -0.43\ V \qquad \text{Eq 1.3}$$

$$CO_2\,(g) + 4H^+ + 4e^- \rightarrow HCHO\,(aq) + H_2O \qquad E^{\circ\prime} = -0.51\ V \qquad \text{Eq 1.4}$$

$$CO_2\,(g) + 6H^+ + 6e^- \rightarrow CH_3OH\,(aq) + H_2O \qquad E^{\circ\prime} = -0.38\ V \qquad \text{Eq 1.5}$$

$$CO_2\,(g) + 8H^+ + 8e^- \rightarrow CH_4\,(g) + 2H_2O \qquad E^{\circ\prime} = -0.24\ V \qquad \text{Eq 1.6}$$

All listed Proton-Coupled Electron Transfer (PCET) reactions (Eqs 1.2-1.6) require less negative potentials than a direct one-electron reduction of CO_2, which requires large reorganization energy between linear CO_2 and $CO_2^{\cdot -}$ (Eq 1.1). Among the above PCET reactions, two-proton and two-electron reduction of CO_2 to CO (Eq 1.2) is

kinetically favorable as well as thermodynamically, in that only one C-O bond is involved during the reaction. On the other hand, a competitive two-electron reduction of H^+ is more favorable at the potential where the Eq 1.2 occurs (Eq 1.7). For this reason, CO_2 reduction catalysts require selectivity toward CO_2 reduction.

$$2H^+ + 2e^- \rightarrow H_2\ (g) \qquad E^{\circ\prime} = -0.42\ V \qquad \text{Eq 1.7}$$

I.3 Coordination Modes of CO_2

There are several different binding modes of CO_2 to transition metals, depending on the number of atoms (η^1 and η^2) or metals (μ^1 and μ^2) involved in coordination. Of them, η^1 and η^2 coordination modes with one metal (μ^1) are discussed below.

The η^2-CO_2 binding mode is explained by using π-orbitals of the C-O bond: σ-bonding from a filled π-orbital on C-O bond to an empty d-orbital of metal, and π-backbonding from a filled d-orbital of metal to antibonding π-orbital on C-O bond. The first molecular structure of CO_2 coordination was observed in $[Ni(CO_2)(PCy_3)_2]\cdot 0.75$toluene, where CO_2 binds as η^2-CO_2 (Figure 1.2).[2] C-O bond distances are 1.22 and 1.17 Å (bond lengths in free CO_2: 1.16 Å), where only one of two C-O bonds is affected by coordination.

CO_2 molecule's dipoles influence the coordination modes of CO_2 to transition metal complexes. A linear, symmetric CO_2 molecule has dipoles on its bonds between carbon and oxygen, resulting in electrophilic carbon and nucleophilic oxygen. A nucleophilic metal center can attack the electrophilic carbon of CO_2 molecule to give a η^1-CO_2 coordinate. Figure 1.3 is an example of the first η^1-CO_2 complex on rhodium.[3]

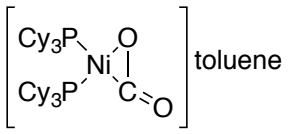

Figure 1.2 η^2-binding mode of CO_2 in $[Ni(CO_2)(PCy_3)_2]\cdot 0.75$toluene. Reproduced from [2].

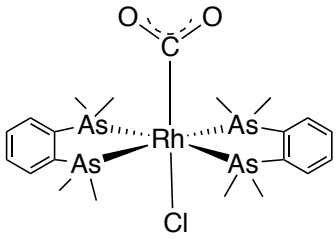

Figure 1.3 η^1-binding mode of CO_2 in $Rh(diars)_2(Cl)(CO_2)$. Reproduced from [3].

C-O bond distances are 1.20 and 1.25 Å, which are longer than those of free CO_2. Both C-O bond lengths are influenced in this mode, while only one of two bonds is affected in η^2 binding mode.

I.4 Relevant CO_2 Reduction Catalysts and Effects of Proton Relays

CO dehydrogenase (CODH) is an example of CO_2 utilizing catalysts found in bacteria, where an electrophilic carbon atom of CO_2 binds to nucleophilic nickel center and the nucleophilic CO_2 oxygen atom binds to an oxophilic iron ion.[4] Besides, adjacent amino acids interact with oxygen atoms by hydrogen bonding and stabilize CO_2 adduct. The additional interactions are important for synthetic catalysts as well.

In I.4.1, previously reported synthetic CO_2 reduction catalysts featuring macrocyclic ligands are discussed to understand how interactions from the secondary

coordination sphere impact reactivity. In I.4.2, Lehn-type pre-catalysts and their proposed mechanisms for CO_2 reduction are reviewed.

I.4.1 Effects of Interactions from the Secondary Coordination Sphere to Improve Catalysis

One of the advantages of molecular catalysts is that their ligands and metal centers can be easily modified. Changing ligands directly attached to a metal center has significant effects on the molecule's properties. In addition, alternations in its secondary coordination sphere would affect the properties as well. Following examples demonstrate improved catalytic activities by changing ligands, which interact with substrates in proximity to stabilize intermediates.

Considering that proton-coupled CO_2 reduction is favored thermodynamically, having proton sources nearby to catalytic sites may improve the reduction processes. Modification of iron tetraphenylporphyrin (FeTDHPP), featuring hydroxyl groups in its secondary coordination sphere is an example of utilizing local proton source for CO_2 re-

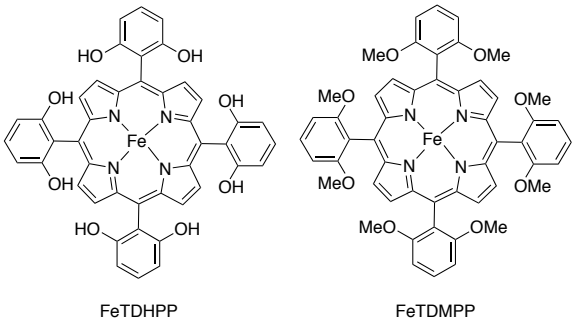

Figure 1.4 Modified FeTDHPP complex. FeTDHPP (left) and FeTDMPP (right). Reproduced from [5].

duction (Figure 1.4).[5] Compared with FeTDMPP featuring methoxy groups instead of hydroxyl groups, FeTDHPP is ~ 1 billion better in terms of turnover frequency (TOF).

In addition to the proximate proton sources as discussed above, hydrogen bonding interactions from the secondary coordination sphere also influence on the catalysis. $Ni(cyclam)^{2+}$ (cyclam = 1,4,8,11-tetrazacyclotetradecane) is a catalyst for a CO_2 reduction, featuring redox inactive macrocyclic ligand (Figure 1.5).[6] One-electron reduced species adsorbed on a mercury electrode react with a CO_2 molecule to give CO as the ultimate product of electrocatalytic CO_2 reduction. The N-H protons of the adsorbed species are facing the same side, and the protons can stabilize the CO_2 adduct by hydrogen bonding depicted in Figure 1.5.

Modifications of the ligand would influence on catalytic systems either directly involving in the reaction or indirectly interacting with the substrates. In Chapter II, our synthetic complex featuring amine group in its secondary coordination sphere is proposed for electrocatalytic CO_2 reduction with anticipated indirect interactions for catalysis.

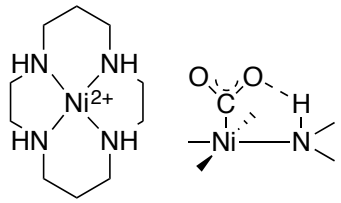

$Ni(cyclam)^{2+}$

Figure 1.5 $Ni(cyclam)^{2+}$ and its interaction with activated CO_2 through N-H proton.

I.4.2 Review of Lehn-Type Catalysts and Their Selectivity Toward CO_2

Lehn-type pre-catalysts, $Re(L)(CO)_3X$ (L = bpy, phen, X = Cl, Br, py), have been studied extensively as CO_2 reduction electrocatalysts since the 1980s. Its distinct characteristics are the selective reduction of CO_2 over H^+ in the presence of protons as well as high catalytic activity. Figure 1.6 provides a general overview of proposed mechanisms for CO_2 reduction for Lehn-type catalysts. At sufficiently negative working potentials, these catalysts follow the uni-molecular mechanism, where two successive one-electron reduced species undergo catalytic reactions after axial chloride ligand dissociation. An addition of proton sources increases catalytic activities, as it undergoes proton-coupled CO_2 reductions (Eq 1.2).

The one-electron reduced species can follow the bi-molecular mechanism as well. This is kinetically less favorable than the uni-molecular mechanism since two

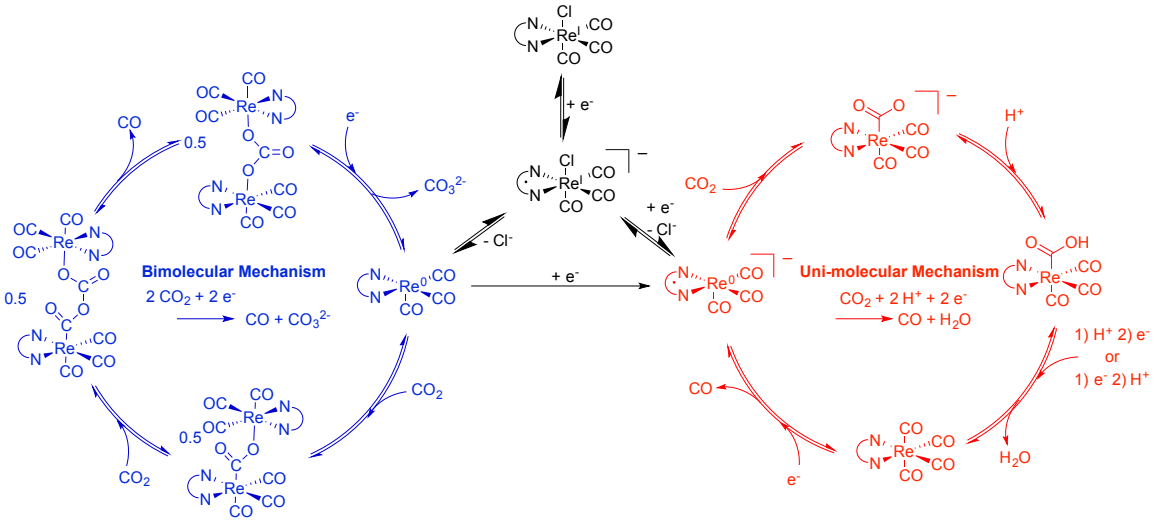

Figure 1.6 Proposed mechanisms for Lehn-type pre-catalysts.

molecules of the active species are involved in the catalytic reaction. On the other hand, the mechanism requires lower overpotential to initiate the catalytic cycle. Re((4,4′-bis(methyl acetamido-methyl)-2,2′-bipyridine)$(CO)_3Cl$ is engineered to feature the amide moiety for hydrogen-bonding between two one-electron reduced active species. The hydrogen-bonded intermediate follows the bi-molecular mechanism at a lower potential than the uni-molecular one.[7,8]

I.5 Conclusions

Utilizing CO_2 as a C1 feedstock can produce chemicals as well as lead to a decrease in the CO_2 levels in the atmosphere. Electrochemical reductions can be carried out to reduce a thermodynamically stable CO_2 molecule. PCET reactions can lower the potential required for catalysis, and interactions between activated CO_2 and functionalities in the secondary coordination sphere would facilitate catalytic reactions.

CHAPTER II

PHENANTHROLINE-BASED RHENIUM TRICARBONYL COMPLEX FEATURING AMINE MOIETIES FOR ELECTROCATALYTIC CO_2 REDUCTION

II.1 Introduction

Lehn-type electrocatalysts display selectivity towards CO_2 over H^+ reduction in the presence of acids. Phenanthroline-based rhenium tricarbonyl complexes were proposed as potential CO_2 reduction molecular catalysts. Modifications in the secondary coordination sphere of these catalysts were investigated in this study. Specifically, complexes of phen-type ligands featuring charged ammonium or amine functional groups ($\mathbf{1}^{2+}$ and **2**, respectively, Figure 2.1) were targeted. The ammonium functionalization was expected to change redox potentials associated with ligand- and metal-based reduction events due to electrostatic considerations, while not altering the electronic structure of the phen-based p and p* system. The incorporation of tertiary amines into the secondary coordination sphere was investigated to test for possible protonation events to feature R_3NH^+ ammonium species, which could act either as intramolecular proton shuttles and/or favor CO_2 binding via CO_2-H-N interactions.

In this chapter, the attempted synthesis of $\mathbf{1}^{2+}$ is described, and synthetic challenges are discussed. Complex **2** was successfully synthesized and its molecular structure was confirmed by single crystal X-ray diffraction.

Catalytic metrics of CO_2 reduction by **2** were compared to the unfunctionalized parent compound **3** featuring methyl groups in the 1,10-positions of phenanthroline. Spe-

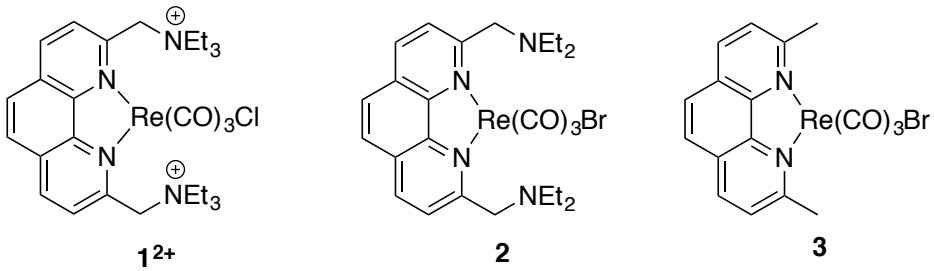

1^{2+} 2 3

Figure 2.1 Schematic of the molecular structures of 1^{2+}, 2, and 3.

ctroelectrochemistry was utilized to explore the electronic structure of the reduced phen-based rhenium tricarbonyl systems. Redox properties of the investigated rhenium complexes were elucidated by means of cyclic voltammetry (CV). As the CO_2 reduction to CO involves two protons ($CO_2 + 2H^+ + 2e^- \rightarrow CO + H_2O$), influences of external proton sources were also examined by the CV technique. Brønsted acids (MeOH, H_2O, TFE and acetic acid) were selected as proton sources for this study. Gas chromatography (GC) was utilized to confirm the gaseous reduction products of Controlled potential electrolysis (CPE).

II.2 Results and Discussion

Ligand $\mathbf{L1^{2+}}$ was directly synthesized from **L0** by heating at 70 ˚C in triethylamine (Scheme 2.1). Anion exchange with saturated NH_4PF_6 aqueous solution precipitated ligand $\mathbf{L1(PF_6)_2}$. Single crystals were formed from slow diffusion of THF into CH_3CN solution of the compound, and the molecular structure of $\mathbf{L1(PF_6)_2}$ was

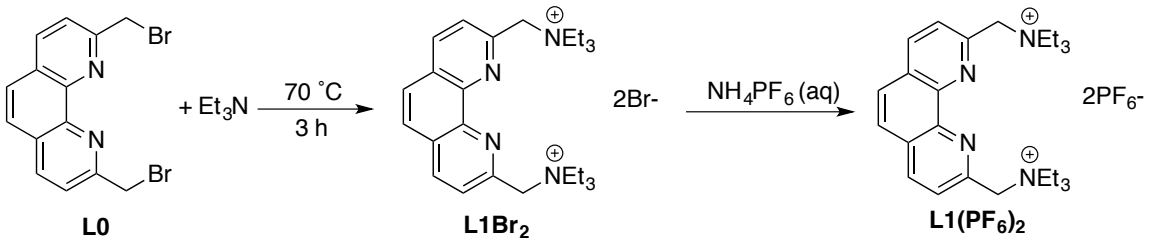

Scheme 2.1 Synthesis of $L1^{2+}$.

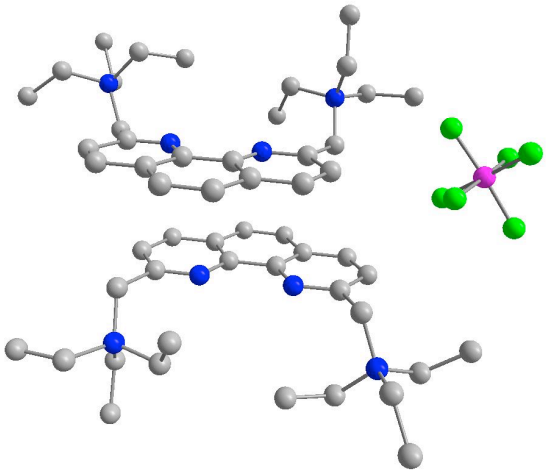

Figure 2.2 Molecular structures of $L1(PF_6)_2$. Green = F, pink = P, blue = N, gray = C. Hydrogen atoms have been omitted for clarity.

obtained from single crystal X-ray diffractometry (Figure 2.2). The ammonium moieties are pointing in the same direction, presumably due to packing effects.

The synthesis of the $Re(CO)_3Cl$ complex of **L1(PF$_6$)$_2$** was attempted following standard preparative protocols for Lehn-type catalysts. However, the reaction of **L1(PF$_6$)$_2$** with $Re(CO)_5Cl$ in toluene at elevated temperatures did not produce the desired product **1(PF$_6$)$_2$** (Scheme 2.2). As an alternative reaction for the synthesis of $\mathbf{1}^{2+}$, we attempted the direct reaction of **4** with trimethylamine (Scheme 2.3). Unfortunately,

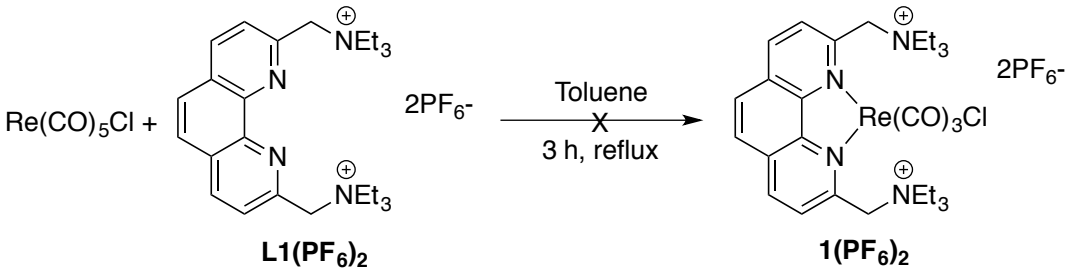

Scheme 2.2 An attempted synthesis of $1(PF_6)_2$ from $Re(CO)_5Cl$ and $L1(PF_6)_2$.

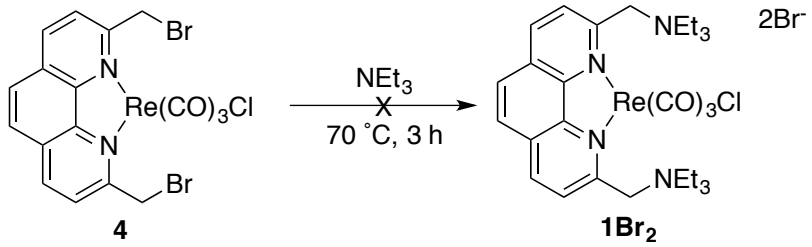

Scheme 2.3 An attempted synthesis of $1Br_2$ from 4 and triethylamine.

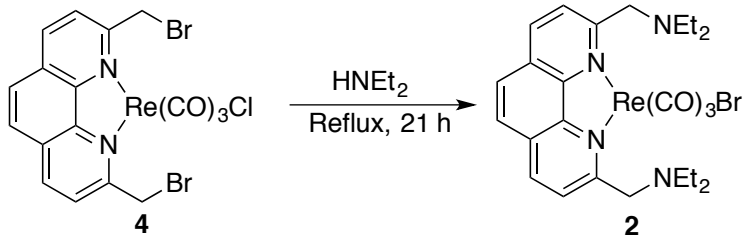

Scheme 2.4 Synthesis of 2 from 4 and diethylamine.

this route did also not yield the desired product. The steric bulk in $\mathbf{L1}^{2+}$, which features three ethyl groups per ammonium N-atom could be the reason for the above observations.

While the preparation of the charged rhenium tricarbonyl complex $\mathbf{1}^{2+}$ was unsuccessful, the amine-functionalized complex **2** was readily obtainable (Scheme 2.4). The reaction of **4** with diethylamine furnished **2** in good yields. During the metallation,

halide exchange was observed, which can be seen in its molecular structure as determined by single crystal X-ray diffractometry (Figure 2.3). Likely, a free bromide generated during the amination steps replaces the axial chloride ligand on the rhenium center.[9] The crystal packing places the two amine moieties facing the same side.

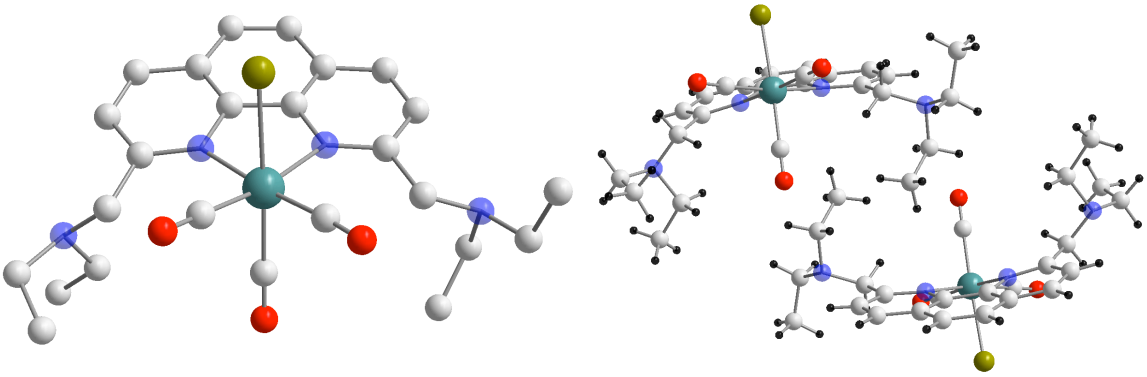

Figure 2.3 Molecular structures of 2. Turquoise = Re, gold = Br, blue = N, red = O, white = C. Hydrogen atoms have been omitted for clarity (left).

Table 2.1 Crystallographic Data for 2

Formula	$C_{25}H_{30}BrN_4O_3Re$
Crystal system	triclinic
Space group	P–1
a, Å	8.3192(12)
b, Å	12.2661(19)
c, Å	13.021(2)
α, °	101.119(5)
β, °	93.977(5)
γ, °	90.099(5)
Volume, Å^3	1300.5(3)
Z	2
T, K	103(2)
ρ_{calcd} (mg/m^3)	1.789
F(000)	684
Θmin, Θmax, °	1.598, 29.383
R_1^a, wR_2^b ($I > 2\sigma(I)$)	0.0502, 0.1451
R_1^a, wR_2^b (all data)	0.0539, 0.1504

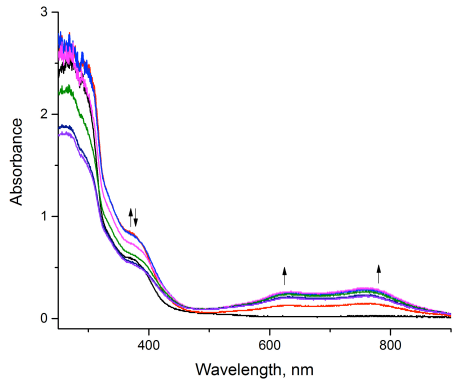

Figure 2.4 UV-Vis absorption spectra of 3 recorded in the course of the reduction with an applied potential of –1.76 V. The first line (black) was recorded without applied potential. Intensity at ~ 380 nm increased immediately, and then decreased with time.

II.2.1 Spectroelectrochemistry

Spectroelectrochemistry was utilized to gain insight into nature of the reduced species of **2** and **3**. The cyclic voltammograms were obtained to find potentials for reduction processes. The CV response of **3** exhibits the first reduction onset potential at –1.50 V (discussed in more detail below). A potential of –1.76 V was applied to detect the first reduced species, and the absorption spectra were recorded during the electrolysis. The absorption spectra during the experiment are shown in Figure 2.4, exhibiting an immediate growth of the band observed at ~ 380 nm during electrolysis. This is in agreement with the previously reported metal-to-ligand-charge transfer (MLCT), specifically an electron transition of $Re(CO)_3Cl \rightarrow$ phen ligand.[10] The broad band(s) at a longer wavelength (600 ~ 800 nm) is in agreement with reduced species of the phen ligand as well. From this experiment, it is concluded that the initial one-

electron reduction of **3** is ligand based, resulting in a species such as $\{[(Phen)(Me)_2]^{\cdot -}$ $Re(CO)_3Cl\}^-$.

The results from spectroelectrochemistry experiments of **2** were similar to those obtained for **3** (Figure 2.5). Based on the CV response of **2**, a potential of –1.91 V was applied to the reduction process. The absorption spectra recorded during the electrolysis have the band at ~ 380 nm which can be assigned to the MLCT transition of $Re(CO)_3Cl$ → phen-based ligand. The broad absorption in 600 ~ 800 nm region is originated from the ligand as observed from the spectroelectrochemistry experiment of **3**.

From the spectroelectrochemistry experiment, we conclude that the initial one electron reduction of both, **2** and **3**, result in phenanthroline centered reduction events, in accordance with previous findings of Lehn-type catalyst systems.

II.2.2 Cyclic Voltammetry Experiments

The CV of **3** under Ar atmosphere has two reduction features at –1.70 V (onset

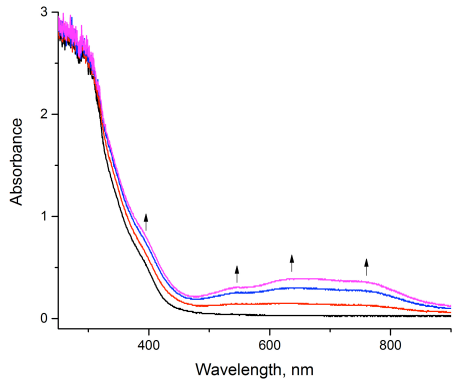

Figure 2.5 UV-Vis absorption spectra of 2 recorded in the course of the reduction with an applied potential of –1.91 V. The first line (black) was recorded without applied potential.

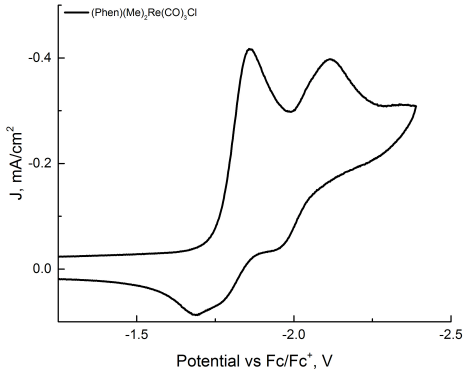

Figure 2.6 Cyclic voltammograms recorded for 1 mM solution of 3 (0.1 M NBu_4PF_6) in CH_3CN under Ar atmosphere at a scan rate of 100 mVs^{-1}.

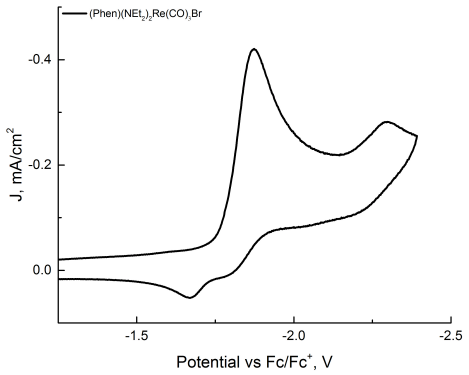

Figure 2.7 Cyclic voltammograms recorded for 1 mM solution of 2 (0.1 M NBu_4PF_6) in CH_3CN under Ar atmosphere at a scan rate of 100 mVs^{-1}.

potential) followed by the second reduction at –1.98 V (onset potential) vs internal Fc/Fc^+ reference (Figure 2.6). The first reduction is quasi-reversible and can be assigned to the reduction of the phenanthroline moiety as discussed above.

The CV response of **2** under Ar atmosphere is recorded, and it has two reduction features at –1.75 V and –2.15 (Figure 2.7). The first reduction potential is similar to that

of **3**. This implies that the modification of the ligand does not affect the first reduction process.

The CV responses of **2** and **3** under CO_2 are shown in Figure 2.8 and Figure 2.9, respectively. For complex **3**, a significant current enhancement at the second reduction potential is observed, while there is no change of the initial reduction event. This observation is in agreement with the traditional Lehn-type catalytic uni-molecular mechanism discussed previously. On the other hand, amine featuring complex **2** displays

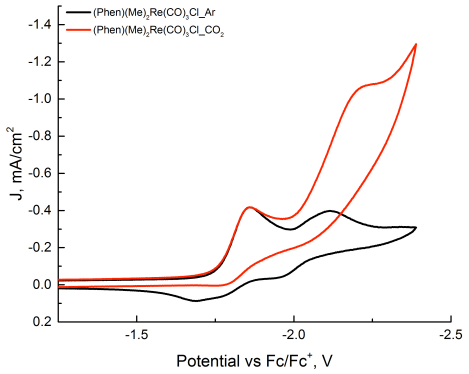

Figure 2.8 Cyclic voltammograms recorded for 1 mM solution of 3 (0.1 M NBu_4PF_6) in CH_3CN under Ar (black) and CO_2 (red) atmosphere at a scan rate of 100 mVs^{-1}.

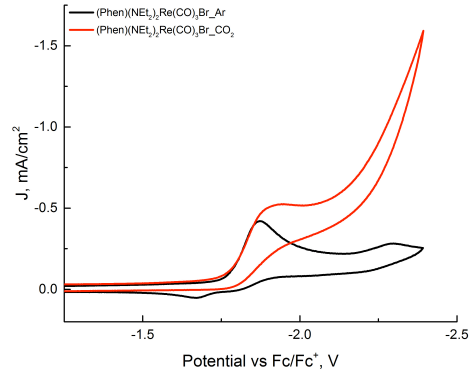

Figure 2.9 Cyclic voltammograms recorded for 1 mM solution of 2 (0.1 M NBu_4PF_6) in CH_3CN under Ar (black) and CO_2 (red) atmosphere at a scan rate of 100 mVs^{-1}.

current enhancement at both reduction potentials. Possibly, the participation of the one-electron reduced species of **2** in the bi-molecular CO_2 reduction mechanism may attribute to the current increment at the first reduction potential (see Figure 1.6)

In order to understand the effect of external proton sources, CVs were recorded with the addition of external proton sources. MeOH, H_2O, TFE, and acetic acid were selected for this study.

II.2.3 CV Responses with MeOH

The CV responses of **3** with an addition of MeOH are shown in Figure 2.10. Under Ar atmosphere, the current remained similar with various MeOH concentrations, from –0.417 mA/cm^2 to –0.530 mA/cm^2 for peak current densities. At high MeOH conc-

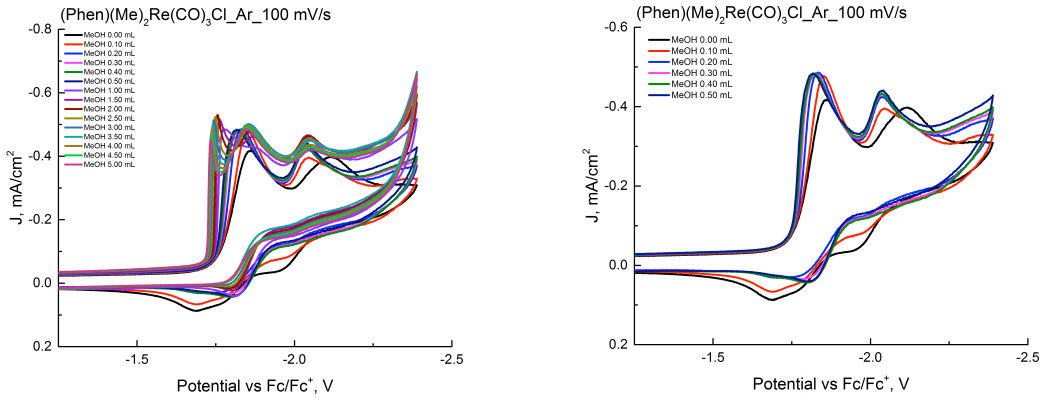

Figure 2.10 Cyclic voltammograms recorded for 1 mM solution of 3 (0.1 M NBu_4PF_6) in CH_3CN under Ar atmosphere with different concentration of MeOH at a scan rate of 100 mVs^{-1}. (right) Selected CV responses from left.

entrations (addition of more than 1.00 mL of MeOH to 10.00 mL of analyte solution in CH_3CN, 9.1%), we observed a new peak at less negative potentials.

The CVs of **3** were next recorded at the same MeOH concentrations under CO_2 atmosphere (Figure 2.11). The CVs feature sigmoidal shapes at lower MeOH concentrations (up to 0.50 mL MeOH addition). As the MeOH concentration increased, the current become peak shapes having a little shoulder at the less negative potentials. The observations of the CV responses under Ar and CO_2 clearly indicate that the additional MeOH affects the current of the reduction waves under CO_2.

The CV responses of **2** under Ar atmosphere are different from that of **3** (Figure 2.12). As the MeOH concentration increases, the first reduction current decreases and a new wave at more negative potentials is observed. The new wave is significant contrary

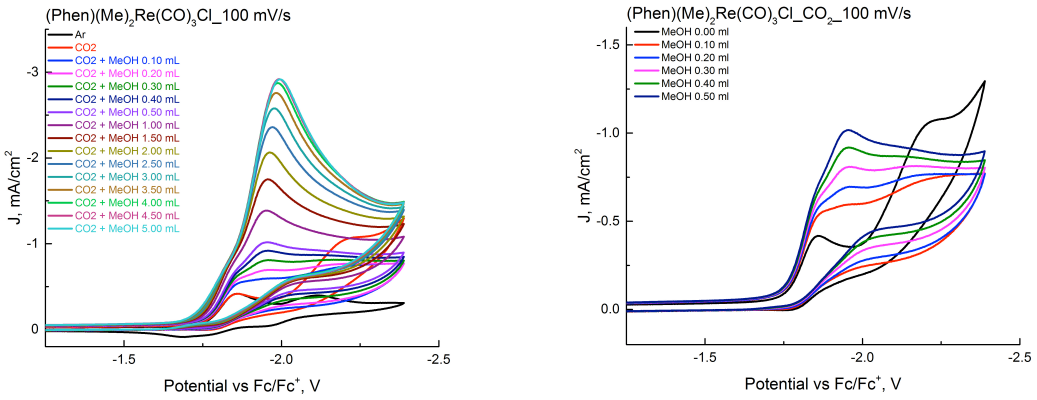

Figure 2.11 Cyclic voltammograms recorded for 1 mM solution of 3 (0.1 M NBu_4PF_6) in CH_3CN under CO_2 atmosphere with different concentration of MeOH at a scan rate of 100 mVs^{-1}. (right) Selected CV responses from left.

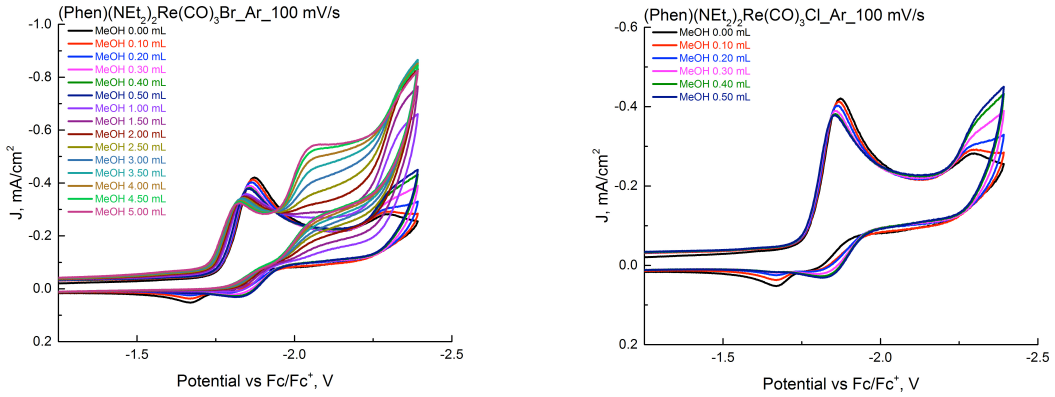

Figure 2.12 Cyclic voltammograms recorded for 1 mM solution of 2 (0.1 M NBu_4PF_6) in CH_3CN under Ar atmosphere with different concentration of MeOH at a scan rate of 100 mVs^{-1}. (right) Selected CV responses from left.

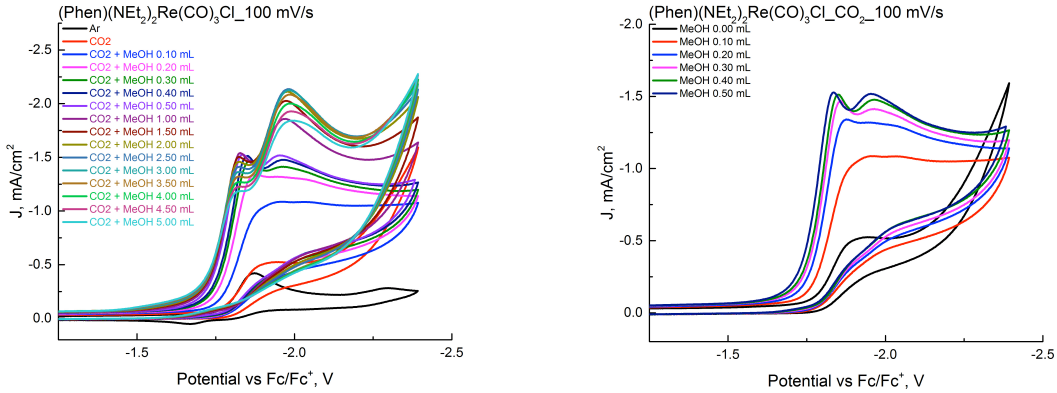

Figure 2.13 Cyclic voltammograms recorded for 1 mM solution of 2 (0.1 M NBu_4PF_6) in CH_3CN under CO_2 atmosphere with different concentration of MeOH at a scan rate of 100 mVs^{-1}. (right) Selected CV responses from left.

to the current density range of **3** (0.113 mA/cm^2). It may imply side-phenomena under the given condition. One possible explanation is that one electron reduced species dimerize at higher concentrations of MeOH, giving rise to the new reduction wave at more negative potential.

Under CO_2 atmosphere, the current of the first reduction potential increases by increasing the MeOH concentration (Figure 2.13). Considering that **2** may undergo bimolecular mechanism ($2CO_2 \rightarrow CO + CO_3^{2-}$) at the first reduction potential (*vide supra*), the proton concentration does not directly influence the catalytic activity. In fact, the first reduction peak reaches its maximum at 1.00 mL MeOH concentration. From the non-linear relationship between the concentration and the peak current, the additional MeOH can be understood as a minor factor helping the first reduction process. Specifically, solvation effects or protonation of the compound would bring two active species (one-electron reduced compound) closely, so that the bimolecular CO_2 reduction process may become facile. The second peak growth at high MeOH concentration is observed as the Ar experiment. The second reduction potential moves to the less negative potential under CO_2 atmosphere, while no significant shift was observed under Ar atmosphere. While the first and the second reduction current densities are similar at low concentrations of MeOH, the difference between the two waves became distinct at higher MeOH concentrations. Assuming that the one-electron reduced species dimerize at high concentrations of MeOH, the current enhancement at the second reduction potential would indicate the dimerization process at the expense of the first reduction process.

II.2.4 CV Responses with H_2O

The CV responses of **3** to the presence of H_2O under Ar atmosphere are similar to that of the MeOH experiments (Figure 2.14). While the shape of the reduction waves looks similar, tre-

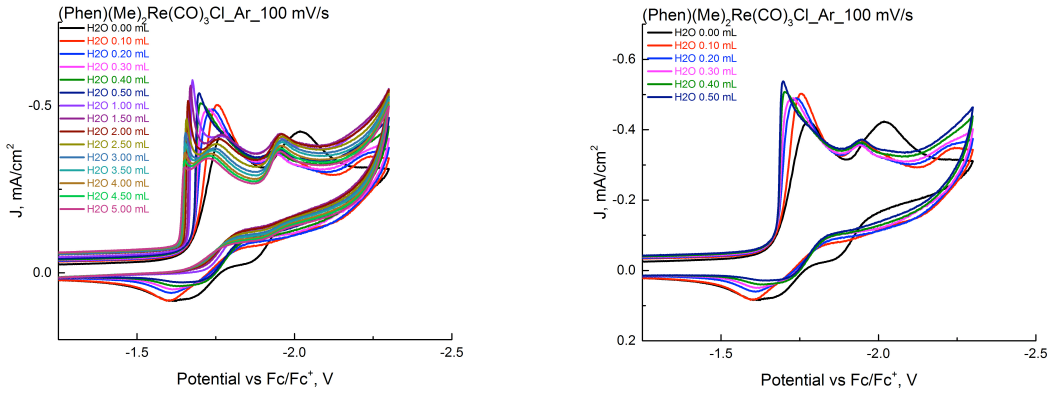

Figure 2.14 Cyclic voltammograms recorded for 1 mM solution of 3 (0.1 M NBu_4PF_6) in CH_3CN under Ar atmosphere with different concentration of H_2O at a scan rate of 100 mVs^{-1}. (right) Selected CV responses from left.

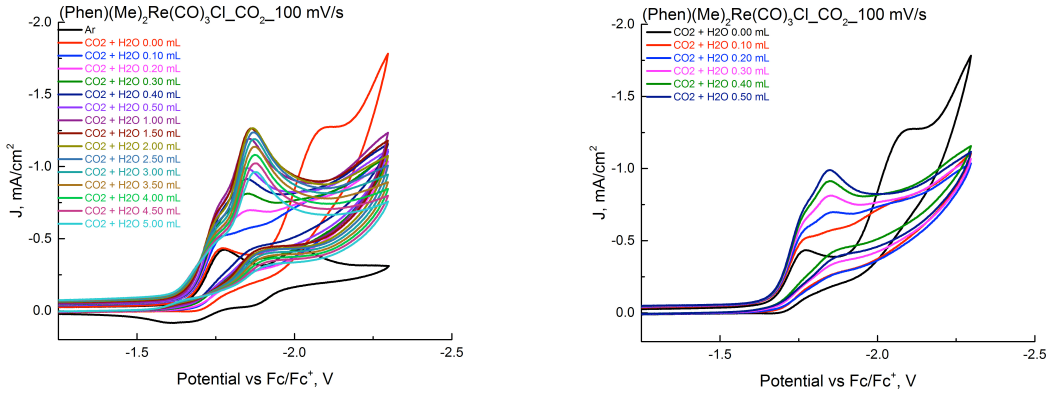

Figure 2.15 Cyclic voltammograms recorded for 1 mM solution of 3 (0.1 M NBu_4PF_6) in CH_3CN under CO_2 atmosphere with different concentration of H_2O at a scan rate of 100 mVs^{-1}. (right) Selected CV responses from left.

nds of their current density were slightly different. The current density with additional MeOH is higher than without MeOH. On the other hand, the current density with additional H_2O decreases more rapidly than that of the MeOH.

The CV responses in the presence of H_2O under CO_2 atmosphere are also similar to those for the corresponding MeOH addition experiment (Figure 2.15). The magnitude

of the current density with the same volume of external acids is lower in the H_2O experiment than the MeOH experiment.

As **3** shows similar reactivity toward MeOH and H_2O, **2** also presents similar CV responses with the two external proton sources (Figure 2.16 and Figure 2.17). One major difference is observed under CO_2 atmosphere: while both acids have two reduction waves, the CV responses in the presence of the MeOH gives a dominant peak growth at

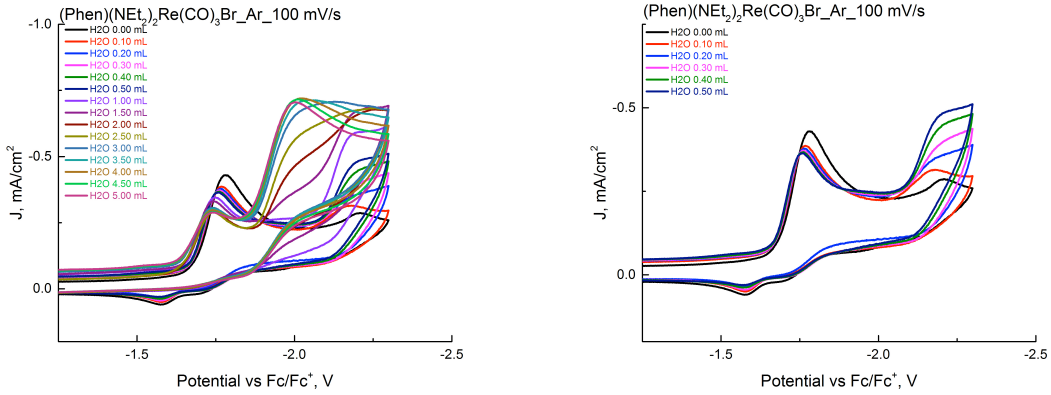

Figure 2.16 Cyclic voltammograms recorded for 1 mM solution of 2 (0.1 M NBu_4PF_6) in CH_3CN under Ar atmosphere with different concentration of H_2O at a scan rate of 100 mVs^{-1}. (right) Selected CV responses from left.

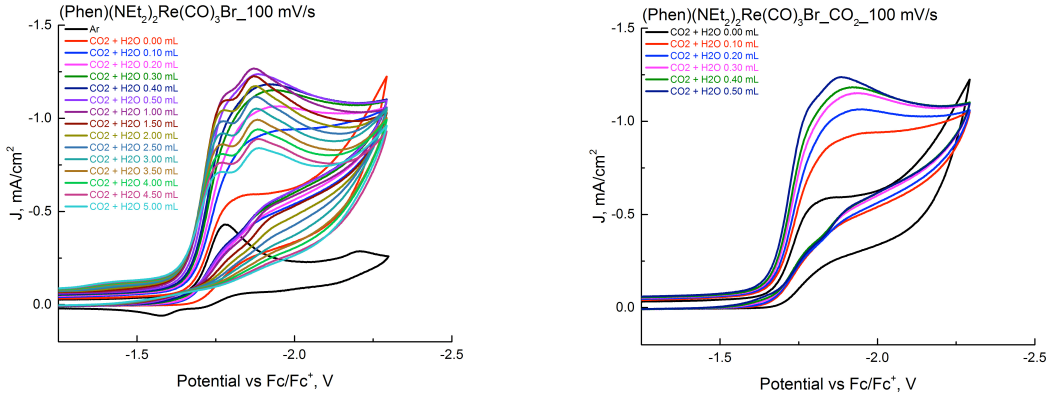

Figure 2.17 Cyclic voltammograms recorded for 1 mM solution of 2 (0.1 M NBu_4PF_6) in CH_3CN under CO_2 atmosphere with different concentration of H_2O at a scan rate of 100 mVs^{-1}. (right) Selected CV responses from left.

the second reduction potential. This difference is surprising as MeOH and H_2O have similar pK_a values in organic solvents and H_2O is typically considered a stronger ligating ligand.

II.2.5 CV Responses with TFE

Since TFE is a stronger acid than MeOH and H_2O, 0.05 mL increments were chosen for the TFE experiments (0.50 mL increments for the MeOH and H_2O experiments). The CVs of **3** under an Ar atmosphere in the presence of TFE display two reduction waves, similarly to our observations for the above described MeOH and H_2O addition experiments (Figure 2.18). However, in this case, there is no new peak growth at less negative potentials, which was observed with a high concentration of MeOH and H_2O. Further investigations are needed to understand whether TFE addition can result in

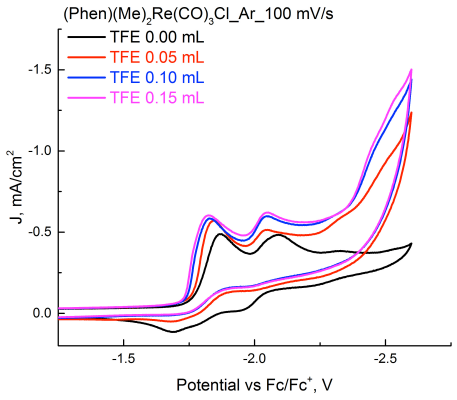

Figure 2.18 Cyclic voltammograms recorded for 1 mM solution of 3 (0.1 M NBu_4PF_6) in CH_3CN under Ar atmosphere with different concentration of TFE at a scan rate of 100 mVs^{-1}.

a new peak growth at higher concentrations.

The CV responses of **3** under CO_2 atmosphere are presented in Figure 2.19. The CVs feature one reduction peak at higher concentration, while there are two reduction waves observed for MeOH and H_2O experiments. It can be attributed to the strong acidity of TFE and solvation effects, decreasing the required potential for the second re-

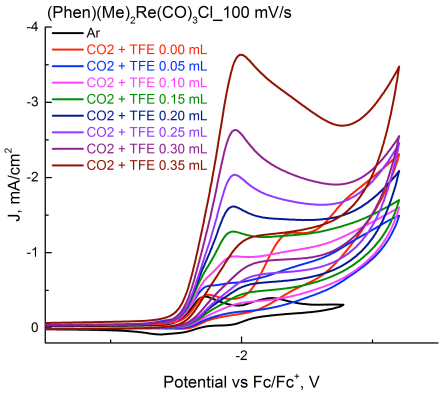

Figure 2.19 Cyclic voltammograms recorded for 1 mM solution of 3 (0.1 M NBu_4PF_6) in CH_3CN under CO_2 atmosphere with different concentration of TFE at a scan rate of 100 mVs^{-1}.

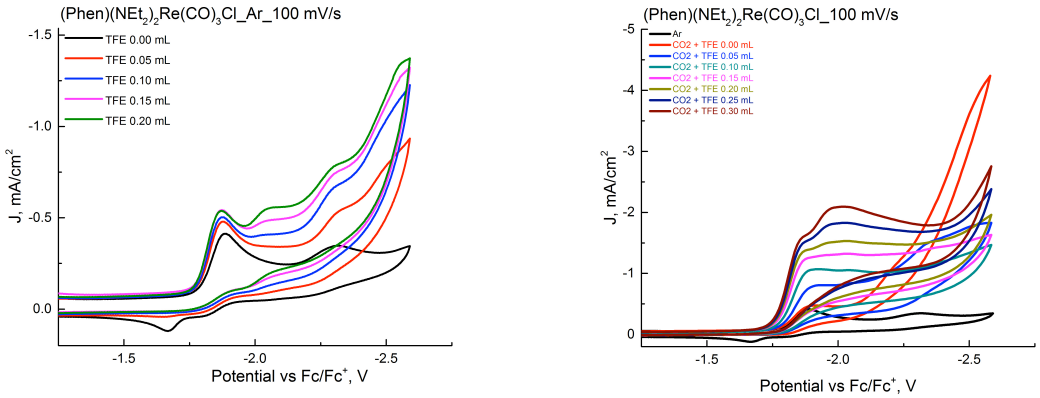

Figure 2.20 Cyclic voltammograms recorded for 1 mM solution of 2 (0.1 M NBu_4PF_6) in CH_3CN under Ar(left) and CO_2(right) atmosphere with different concentration of TFE at a scan rate of 100 mVs^{-1}.

duction. The second reduction potential becomes less negative by increasing the amount of TFE, and then the second reduction may occur at the first reduction potential.

As **3** has similar CV responses with TFE compared with MeOH and H_2O, a choice of acids did not affect the CV responses of **2** (Figure 2.20). A difference comes from the different strengths of acids, resulting in immediate CV responses with small amounts of TFE.

II.2.6 CV Responses of 2 in the Presence of Acetic Acid

While weak Brønsted acids result in similar CV responses, the presence of acetic acid shows significantly different features. Under Ar atmosphere, reduction waves shift from –1.75 V to –1.40 V or less in the presence of acetic acid (Figure 2.21). While weak Brønsted acids shift reduction potentials slightly with the similar reduction features, the

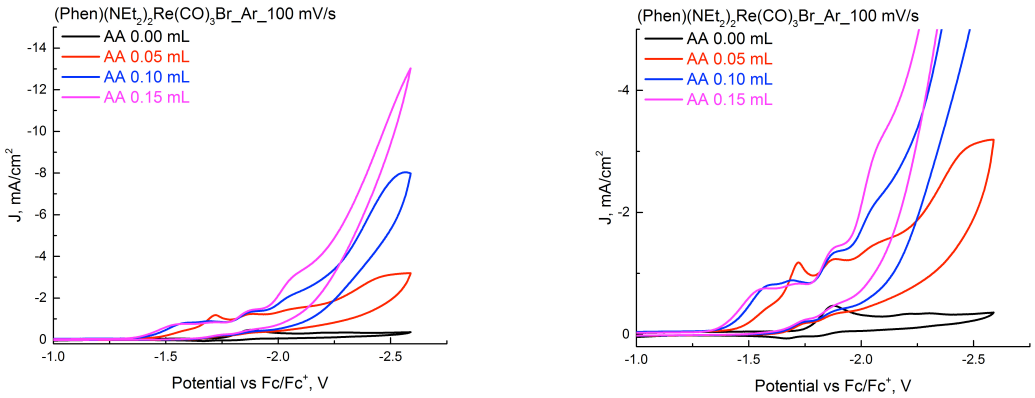

Figure 2.21 Cyclic voltammograms recorded for 1 mM solution of 2 (0.1 M NBu_4PF_6) in CH_3CN under Ar atmosphere with different concentration of acetic acid at a scan rate of 100 mVs^{-1}. (right) A zoomed plot of the left.

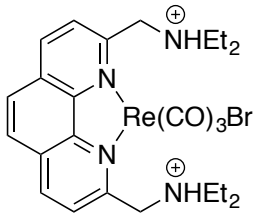

5

Figure 2.22 Proposed protonated species 5.

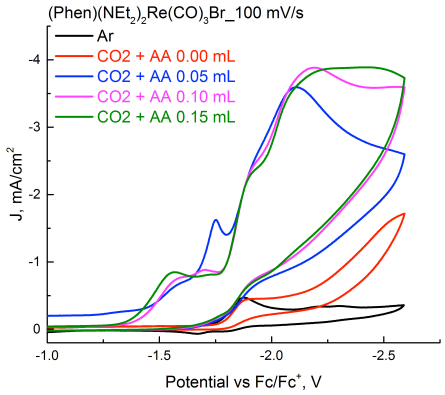

Figure 2.23 Cyclic voltammograms recorded for 1 mM solution of 2 (0.1 M NBu_4PF_6) in CH_3CN under CO_2 atmosphere with different concentration of acetic acid at a scan rate of 100 mVs^{-1}.

CV responses in the presence of acetic acid are totally different from the CV responses in the absence of acetic acid. We propose that the stronger acid may protonate the amine of **2** to positively charged species **5**, then **5** can be reduced at less negative potentials (Figure 2.22)

Interestingly, the CV responses and the current densities measured under CO_2 atmosphere are not significantly different from that of Ar experiment (Figure 2.23). Besides the proposed hypothesis of the protonation of **2**, the electrochemical reduction may undergo different chemical reactions (such as reductions of H^+) instead of the CO_2

reduction and shows the similar current density under Ar and CO_2 atmosphere. Further investigation is needed to confirm the protonation species.

II.2.7 Controlled Potential Electrolysis

Controlled potential electrolysis (CPE) was carried out to verify reaction products observed as current enhancements in the CV responses (*vide supra*). A solution of 1 mM catalyst and 0.1 M $TBAPF_6$ in CH_3CN was saturated with CO_2 atmosphere. As a choice of an acid, 2.50 mL of H_2O (2.64 M) was added to a cell. A potential of –2.10 V was selected for electrolysis potential, which is sufficiently negative for the first reduction process. The electrolysis started with around –3.5 mA of current (Figure 2.24).

However, the current response decreased quickly, and the current became steady near –0.1 mA. During the electrolysis (1200 s), the charge passed was –0.474 C, which implies that there was almost no reaction carried out (Figure 2.25). Gaseous products an-

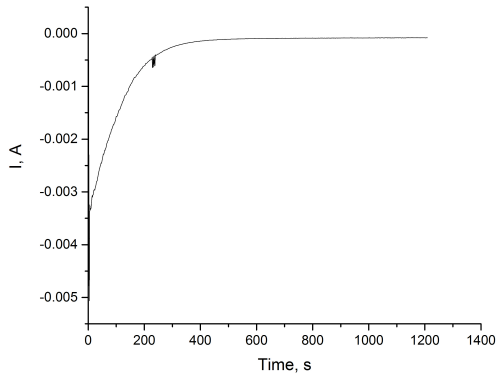

Figure 2.24 A plot of current vs time during electrolysis of 2.

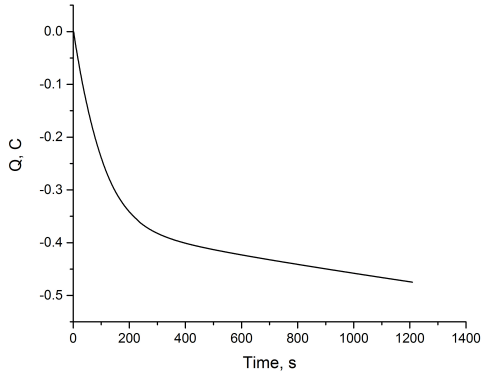

Figure 2.25 A plot of charge passed vs time during electrolysis of 2.

alysis with GC also supports this argument, detecting a small amount of CO, which is too small to be quantified with the current gas chromatography setup.

While the redox reaction of **2** was stable during the CV experiments, the compound was unstable during the electrolysis experiments. The different reactivity can be originated from the difference of the techniques. During the CV experiments, potentials are applied to the system through a small area of the working electrode for a short time. On the other hand, the CPE experiment utilizes a constant applied potential through a large area of the working electrode for a long time.

While there is no obvious reason for the low activity of **2**, decomposition of the compound is a possible reason for the low activity. In addition, the decomposition residue may interfere with the working electrode's activity by interrupting electron transfer kinetics from the electrode to homogeneous catalyst species.

II.3 Conclusions

Complexes $\mathbf{1}^{2+}$ and **2** were proposed as potential electrochemical CO_2 reduction catalysts. While $\mathbf{L1}^{2+}$ was easily obtained, synthesis of $\mathbf{1}^{2+}$ was unsuccessful, partially because of the ligand's bulkiness and possibly due to the positive charges. Complex **2** was successfully isolated from direct amination of complex **4**, with concomitant halide ion exchange.

Spectroelectrochemistry was utilized to investigate electronic transitions in the reduced species of **2**. Comparison with the unfunctionalized parent complex **3** gave similar spectroscopic results, suggesting that the first reduction process is not altered by ligand modification on its secondary coordination sphere.

CV experiments were performed to examine redox activities of **2** under Ar and CO_2 atmosphere, and compared with **3**. While the CV response of **3** has catalytic activities at the second reduction potential as most Lehn-type catalysts, **2** has a reactivity toward CO_2 at the first reduction potential as well. The one-electron reduced species is assumed to follow the bi-molecular mechanism.

As proton-coupled CO_2 reduction is thermodynamically favored than direct CO_2 reduction, effects of external proton sources were examined. In the presence of weak Brønsted acids (MeOH and H_2O), the current enhancements were observed for both potentials of **2**. The first reduction process may follow bi-molecular mechanisms, in that the current densities do not increase linearly by the acid addition. Instead, the acid may have indirect effects on the reduction.

Utilizing acetic acid for the external proton sources results in significantly different CV responses. It is hypothesized that **2** is protonated under this condition to generate **5**, which has doubly protonated amine moieties. Besides, **2** may undergo different chemical reactions under the given experimental condition. Further investigation is needed to prove the hypotheses.

CPE experiment was performed to verify electrochemical reduction products. Complex **2** became deactivated quickly under the chosen conditions. Only trace amounts of CO could be detected by GC, which cannot be quantified to define catalytic activities.

II.4 Experimental

II.4.1 Methods and Materials

Unless otherwise specified, all of the reactions were carried out using Schlenk line under a N_2 atmosphere or a glove box under an Ar atmosphere. All commercially available reagents were used as received. **L0** was synthesized as previously reported.[11] NMR spectra were recorded on either a Mercury 300 MHz or an Inova 500 MHz spectrometer.

II.4.2 Spectroelectrochemistry

A reduction was performed at room temperature under Ar atmosphere in CH_3CN in a Honeycomb quartz cuvette (1.00 cm X 1.00 cm). The electrolysis potential was controlled with an Interface 1000E or a Reference 600 potentiostats from the Gamry

Instruments. UV-Vis spectra were recorded using a DH-2000-BAL light source and an USB2000+XR1-ES spectrophotometer.

II.4.3 Electrochemistry

Electrochemical experiments were performed using either an Interface 1000E or a Reference 600 potentiostats from Gamry Instruments. A cell was used for all cyclic voltammetry experiments with a glassy carbon working electrode (3.0 mm diameter from BASi), graphite counter electrode (6.3 mm graphite rod from Alfa Aeser), and an $Ag/AgNO_3$ non–aqueous reference electrode with internal Fc/Fc^+ as an internal reference. All electrochemical experiments were performed with 0.1 M tetrabutylammonium hexafluorophosphate ($TBAPF_6$) as supporting electrolyte in MeCN. Re complex concentration was 1 mM, and all solutions were purged with Ar or CO_2 before CVs were taken.

II.4.4 Synthesis of 4

100 mL of toluene was added to a flask with 0.112 g of $Re(CO)_5Cl$ (0.298 mmol) and 0.0941 g of **L0** (0.257 mmol). The reaction mixture was refluxed for 2 h. While heating, all solid starting materials were dissolved into solution and color changed from light yellow color to orange color suspension. The supernatant was decanted and the residue was washed with hexanes. The residue was dried under vacuum overnight and 0.104 g of yellow solid was obtained (0.151 mmol, 50.8%). ^1H NMR (300 MHz, DMSO-d_6): δ 8.97 (d, 2H), δ 8.37 (d, 2H), δ 8.30 (s, 2H), δ 5.45 (m, 4H)

II.4.5 Synthesis of 2

1.11 g of **4** (1.62 mmol) was added to a flask with 100 mL of diethylamine. The yellow suspension was refluxed for 25 hours. The brown color solution with dark yellow precipitate was filtered and washed with hexanes. The brown filtrate was reduced under vacuum and 0.702 g (1.05 mmol, 64.6%) of dark brown residue was obtained. The solid was dissolved in toluene, filtered and recrystallized to give dark yellow color solid. ^{1}H NMR (300 MHz, DMSO-d_6): δ 8.83 (d, 2H), δ 8.36 (m, 2H), δ 8.19 (d, 2H), δ 4.38 (m, 4H), δ 2.64 (m, 8H), δ 1.03 (t, 12H)

II.4.6 Synthesis of L1$(PF_6)_2$

0.509 g of **L0** (1.39 mmol) was added to a flask with 20 mL of triethylamine. The suspension was heated at 70 ˚C for 3 hours. The lilac color suspension was filtered. The filtered solid was dried overnight and changed to dark green color. The solid was dissolved in water and added to a saturated NH_4PF_6(aq) solution in drops. The cloudy solution was filtered and the solid was dried overnight (0.917 g, 1.29 mmol, 92.6%). ^{1}H NMR (300 MHz, DMSO-d_6): δ 8.71 (m, 2H), δ 8.17 (s, 2H), δ 8.02 (m, 2H), δ 4.89 (m, 4H), δ 3.51 (m, 12H), δ 1.38 (m, 18H)

II.4.7 Attempted preparation of 1^{2+}

To a flask with 48.3 mg of $Re(CO)_5Cl$ (0.129 mmol) and 86.5 mg of **L1**$(PF_6)_2$ (0.124 mmol), 25 mL of toluene was added. The reaction mixture was refluxed for 3 h under dark. The supernatant was decanted and the residue was washed with hexanes. All

volatiles were removed under vacuum and residue was taken for ^{1}H NMR. No reaction occurred by ^{1}H NMR.

As an alternative way, 0.104 g of **4** (0.151 mmol) was added to 20.0 mL of triethylamine (947 equiv, 143 mmol). The reaction mixture was degassed for 15 min and heated at 70 ˚C for 3 h. The reaction mixture was filtered and water was added to the solid. The solid was not dissolved into water. The solid was taken for ^{1}H NMR. No reaction occurred by ^{1}H NMR.

CHAPTER III

ATTEMPTED SYNTHESIS OF A RHENIUM COMPLEX OF MODIFIED *APYHIST* LIGAND: INTRAMOLECULAR CYCLIZATION OF LIGAND

III.1 Introduction

It is crucial for Lehn-type CO_2 reduction electro-catalysts to feature a redox-active moiety. A pyridine-2,6-diimine ligand scaffold derived from diacetylpyridine was considered as a good candidate for synthetic catalysts, in that it is a non-innocent ligand (Figure 3.1).[12] Previously, a series of ligands modified from the pyridine-2,6-diimine was examined for electrocatalytic reduction of CO_2.[13,14] From their systematic examination, Abruña *at al.* found that the complexes with modified DAPA (DAPA = 2,6-bis-[1-(phenylimino)ethyl]pyridine) have catalytic activities toward a CO_2 reduction in non-aqueous solution (Figure 3.1). The degree of catalytic activities was dependent on the ligand as well as the metal center.

Recognizing the redox activity of the pyridine-2,6-diimine ligand scaffold, we

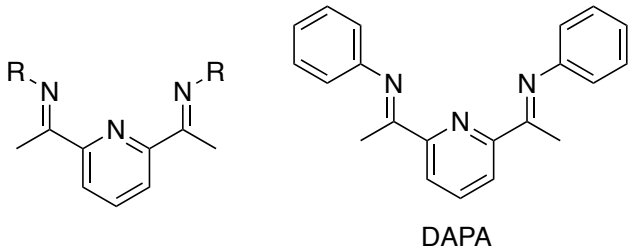

Figure 3.1 (Left) Pyridine-2,6-diimine ligand scaffold, (right) DAPA (2,6-bis-[1-(phenylimino)ethyl]pyridine) ligand.

proposed a rhenium complex featuring ligand **L1** for a potential electro-catalyst for CO_2 reduction (Figure 3.2). The ligand **L1** was designed to incorporate imidazolium moieties, expecting interactions between the imidazolium and a CO_2 adduct would enhance the catalytic activity by stabilizing an intermediate. In the interest of synthetic ease, the *apyhist* ligand scaffold (*apyhist* = 2-(1H-imidazol-4-yl)-N-(1-(pyridin-2-yl)ethylidene)ethanamine) was chosen in this study (Scheme 3.1). Alkylation of the imidazole moiety would generate the desired ligand **L2'** (R = ethyl). Coordination onto rhenium would give a complex featuring an imidazole moiety in the secondary coordination sphere (Figure 3.3).

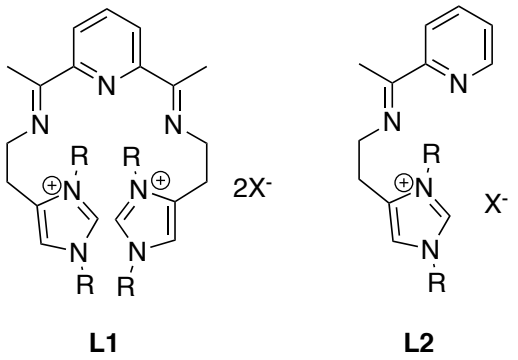

Figure 3.2 The proposed ligands L1 (left) and L2 (right).

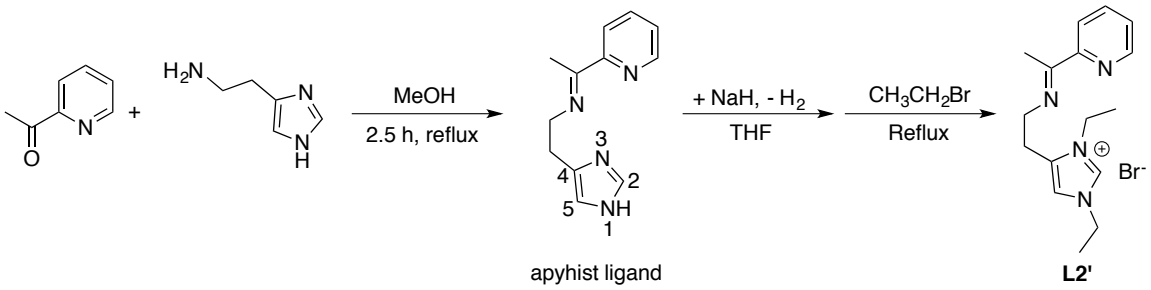

Scheme 3.1 The proposed synthesis of the *apyhist* ligand and L2' from 2-acetylpyridine and histamine.

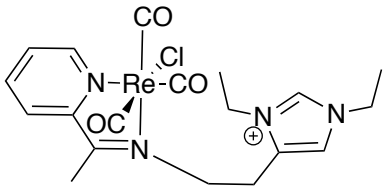

Figure 3.3 The proposed rhenium complex featuring L2'.

III.2 Results and Discussion

Schiff base condensation reaction of 2-acetylpyridine and histamine was anticipated to give the *apyhist* ligand (Scheme 3.1). A copper (II) complex of the *apyhist* ligand was previously reported in which the *apyhist* acts as a tridentate ligand.[15] The preparation of the imidazolium moiety in the proposed ligand **L2'** would require stepwise alkylation of the imidazole group in N1 and N3 positions, as discussed above. The latter would be expected to be challenging if N3 is coordinated to a metal ion. Therefore, we attempted to synthesize the *apyhist* ligand and alkylate it directly.

Previously reported Schiff base condensation reactions of histamine with 2-acetylpyridine or 2,6-diacetylpyridine were carried out followed by *in situ* complexation steps.[16] Presuming the given condition would work for the *apyhist* ligand synthesis as well, histamine and 2-acetylpyridine were refluxed in MeOH (Scheme 3.2). Subsequently, the product was deprotonated and alkylated at N1. Attempted second alkylation on N3 was unsuccessful based on ^{1}H NMR, in which signals corresponding to the presence of an additional ethyl group were not detected (Figure 3.4).

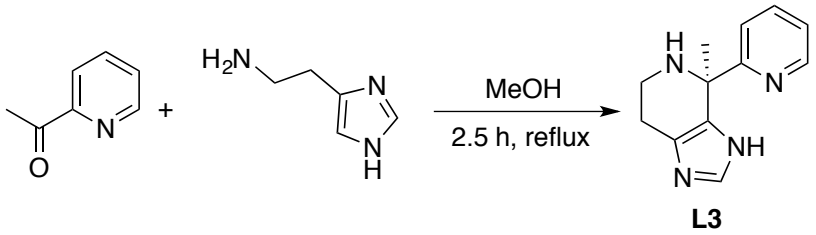

Scheme 3.2 The synthesis of L3 from 2-acetylpyridine and histamine.

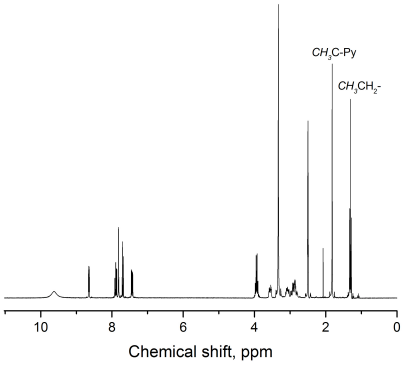

Figure 3.4 ^{1}H NMR spectrum after the attempted alkylation of L3.

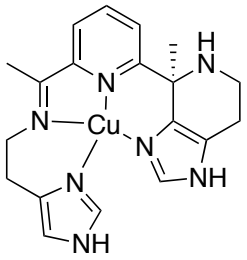

Figure 3.5 Schematic of the molecular structure of the [Cu(I)(imidH)(imidH)'DAP]$^{+}$. Reproduced from [19].

From thorough literature study, few examples of intramolecular cyclization of Schiff base were found. Those examples feature histidine[16–18] or histamine[19–21] moieties in their molecules, resulting in a new C-C bonding between C5 of imidazole moiety and the carbon atom of imine. Interestingly, the rearrangement of the ligand occurs within a

transition metal complex as well. To our knowledge, there is only one example of intramolecular cyclization of Schiff base in a complex form; $[Cu(I)(imidH)_2DAP]^+$ became $[Cu(I)(imidH)(imidH)'DAP]^+$ after few days (Figure 3.5).[19] We assume that the ligand underwent a similar rearrangement. Scheme 3.3 presents a proposed mechanism for the rearrangement.

The ligand **L3** underwent a complexation with rhenium. **L3** was refluxed with $Re(CO)_5Cl$ in toluene and a gray solid was obtained from the mixture. A saturated $CHCl_3$ solution of the compound layered with hexanes gave X-ray quality white crystals, compound **1** (Figure 3.6).

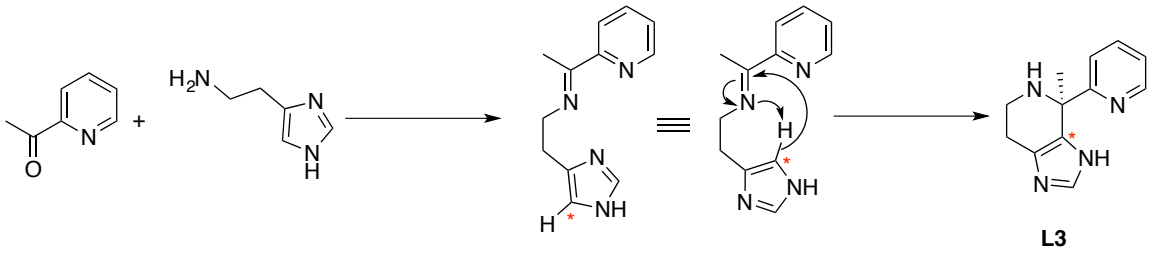

Scheme 3.3 Proposed mechanism of ligand arrangement.

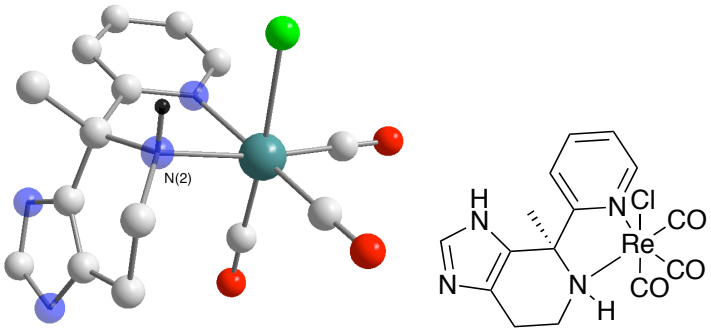

Figure 3.6 (Left) Molecular structure of 1. Turquoise = Re, green = Cl, red = O, blue = N, white = C. Hydrogen atoms have been omitted for clarity except N2-H. Distances: Re-N_{py} 2.162(3) Å; Re-N2 2.214(3) Å. (right) Schematic of the molecular structure of 1.

Table 3.1 Crystallographic Data for $1 \cdot H_2O$

Formula	$C_{15}H_{15}ClN_4O_3Re$, H_2O
Crystal system	triclinic
Space group	P–1
a, Å	8.8136(3)
b, Å	9.0280(3)
c, Å	11.9671(4)
α, °	106.6308(16)
β, °	92.6573(17)
γ, °	109.0821(16)
Volume, $Å^3$	851.89(5)
Z	2
T, K	103(2)
ρ_{calcd} (mg/m^3)	2.208
F(000)	529
Θmin, Θmax, °	1.798, 29.321
$R_1{}^a$, $wR_2{}^b$ ($I > 2\sigma(I)$)	0.0250, 0.0569
$R_1{}^a$, $wR_2{}^b$ (all data)	0.0301, 0.0595

The molecular structure in Figure 3.6 seems a structural isomer from rearrangement reaction. The new C-C bond is clearly shown in its molecular structure. The new N2-H bond formation is inferred from the tetrahedral geometry of the nitrogen atom. Interestingly, the ligand binds to the metal center through two nitrogen atoms. While the cyclized ligand coordinates to the copper (I) ion through the imidazole moiety in $[Cu(I)(imidH)_2DAP]^+$, the cyclized ligand **L3** in **1** coordinates through amine N2. The C_{sp2} of the imine became C_{sp3} after the rearrangement, and a rotation around C_{sp3}-C_{py} bond allows the rhenium (I) ion to achieve an octahedral geometry.

III.3 Conclusions

The *apyhist* ligand scaffold **L3** was selected for a potential CO_2 reduction catalyst. At earlier synthetic steps, we found that a new C-C bond between C5 of the imidazole moiety and carbon atom of imine was made by intramolecular cyclization. The mechanism of the rearrangement was proposed, *vide supra* (Scheme 3.3). Since the imidazole moiety was designed to support the CO_2 reduction by interactions within close distance, the cyclization isomer was no longer useful for a new CO_2 catalyst synthesis. Realizing the C5 is the origin of the cyclization, one could avoid the isomerization by using 4-Methylhistamine(2-(5-methyl-1H-imidazol-4-yl)ethanamine), featuring a methyl group at the C5 position.[22]

III.4 Experimental

III.4.1 Methods and Materials

Unless otherwise specified, all of the reactions were manipulated using Schlenk line under a N_2 atmosphere or a glove box under an Ar atmosphere. All commercially available reagents were used as received. NMR spectra were recorded on either a Mercury 300 MHz or an Inova 500 MHz spectrometer.

III.4.2 Synthesis of L3

3.10 g of histamine (27.9 mmol) and 3.00 mL of 2-acetylpyridine (26.7 mmol) was added to a flask. The reaction mixture was heated at 120 ˚C for 2.5 h. Once it cooled down to room temperature, the brown residue was washed with Pet. Ether. The washes

were decanted. MeOH was added to the flask and the residue was dissolved in MeOH by sonication. Solvent was removed and the brown residue was purified *via* flash chromatography with MeOH and Ethyl acetate mixture on a silica column using Teledyne ISCO's CombiFlash® Rf+ to obtained a light orange color solid (4.68 g, 81.7%). The product is hygroscopic at room temperature. ^{1}H NMR (500 MHz, DMSO-d_6): δ 8.53 (d, 1H), δ 7.80-7.10 (m, 4H), δ 3.02-2.25 (m, 4H), δ 1.52 (s, 3H), aromatic N-H proton was found at downfield.

III.4.3 Attempted alkylation of L3

0.133 g of NaH (5.56 mmol) was dissolved in 40 mL of anhydrous THF. To the cloudy solution, 0.775 g of (3.62 mmol) of **L3** was added and the solution became light yellow suspension. The reaction mixture was refluxed for 15.5 h, and the bubble was evolved during the reaction. The pink color solution was cooled down to room temperature and stirred under N_2 for one day. 260 μL of bromoethane (3.51 mmol) was added to the reaction mixture and refluxed for 19 h. After cooled to room temperature, the orange color suspension was filtered through a fritted funnel and washed with THF. The filtrate was reduced under vacuum and the orange color oil was dissolved in MeOH and washed with hexanes. The MeOH layer was collected and reduced under vacuum. The crude product was used for the next reaction without purification. ^{1}H NMR (300 MHz, DMSO-d_6): δ 8.53 (d, 1H), δ 7.69-7.12 (m, 4H), δ 3.96-3.75 (m, 2H), δ 3.22-2.85 (m, 2H), δ 2.66-2.36 (m, 4H), δ 1.50 (s, 3H), δ 1.29 (t, 3H)

III.4.4 Synthesis of 1

To a flask with 0.234 g of **L3** (1.09 mmol) and 0.405 g of $Re(CO)_5Cl$ (1.12 mmol), toluene was added. The reaction mixture was refluxed for 24 h and reduced under vacuum. The gray color residue was obtained and purified *via* flash chromatography with MeOH and Ethyl acetate mixture on a silica column using Teledyne ISCO's CombiFlash® Rf+ to obtained an off-white solid was obtained (0.0855 g, 15.1%). White crystals formed from a saturated solution of **1** layered with hexane. ^1H NMR (500 MHz, DMSO-d_6): δ 12.04 (s, 1H), δ 8.63 (d, 1H), δ 8.08-8.20 (m, 1H), δ 8.03 (d, 1H), δ 7.52 (t, 1H), δ 7.37-7.38 (m, 1H), δ 5.10 (br. s, 1H), δ 3.72-3.87 (m, 1H), δ 2.98-3.13 (m, 1H), δ 2.87 (dd, 1H), δ 1.82-1.95 (m, 3H)

CHAPTER IV

SUMMARY

CO_2, a final combustion product of hydrocarbons, absorbs Infrared radiation from the sun and causes the greenhouse effect with its high level of CO_2 in the atmosphere. As a means of reducing the level in the atmosphere, conversions of CO_2 to other chemicals have been explored. Among them, electrochemical reduction of CO_2 to CO is of our interest.

Our approach is developing a molecular catalyst suitable for electrochemical CO_2 reduction. Benchmarking the Lehn-type catalysts, we successfully synthesized and characterized **2**, a rhenium tricarbonyl complex featuring amine moieties. **2** was compared with a parent compound **3** in order to investigate effects of the presence of amine moieties. Spectroelectrochemistry results confirmed that the first reductions of both compounds occur in phenanthroline ligand. This concludes that the electronic structure of the phen-based p and p* system is not changed by incorporating the amine moieties.

The CV experiments of **2** and **3** were performed to investigate current changes depending on applied potentials. Both complexes showed current enhancements under CO_2 atmosphere compared with Ar atmosphere. Based on the CV responses of **2** where current enhancements occur at both reduction potentials, **2** may undergo the bimolecular mechanism.

The presence of external proton sources including MeOH, H_2O, TFE, and acetic

acid affects their CV responses. In addition, CPE experiment in the presence of H_2O and its product analysis suggest that side reaction may be predominant than CO_2 reduction. Further research is needed to understand which reaction causes such electric responses and its mechanism.

In Chapter III, the proposed molecular catalyst featuring modified *apyhis*t ligand for CO_2 reduction was discussed. In its synthetic steps, we found that the desired compound was not obtained due to its intramolecular cyclization. In order to prevent such a side reaction, one may utilize 4-methylhistamine instead of histamine.

In summary, electrochemical reduction of CO_2 is a way to decrease the level of CO_2 in the atmosphere as well as to transform it into valuable chemicals. While a direct one-electron reduction of CO_2 requires high overpotential, multi-electron reduction processes need less overpotentials. Along with the multi-electron process, one can exploit molecular catalysts, such as $Ni(cyclam)^{2+}$ and Lehn-type catalysts. Incorporation of amine moieties in their ligand structures may improve catalytic activities facilitated by interactions between substrates and the moieties. Understanding of the interaction is crucial for developing a new system for electrocatalytic CO_2 reduction.

REFERENCES

(1) Appel, A. M.; Bercaw, J. E.; Bocarsly, A. B.; Dobbek, H.; DuBois, D. L.; Dupuis, M.; Ferry, J. G.; Fujita, E.; Hille, R.; Kenis, P. J. A.; Kerfeld, C. A.; Morris, R. H.; Peden, C. H. F.; Portis, A. R.; Ragsdale, S. W.; Rauchfuss, T. B.; Reek, J. N. H.; Seefeldt, L. C.; Thauer, R. K.; Waldrop, G. L. Frontiers, Opportunities, and Challenges in Biochemical and Chemical Catalysis of CO_2 Fixation. *Chem. Rev.* **2013**, *113* (8), 6621-6658.

(2) Aresta, M.; Nobile, C. F.; Albano, V. G.; Forni, E.; Manassero, M. New Nickel-carbon Dioxide Complex: Synthesis, Properties, and Crystallographic Characterization of (Carbon Dioxide)-Bis(tricyclohexylphosphine)nickel. *J. Chem. Soc. Chem. Commun.* **1975**, 15, 636-637.

(3) Calabrese, J. C.; Herskovitz, T.; Kinney, J. B. Carbon Dioxide Coordination Chemistry. 5. The Preparation and Structure of the Rhodium Complex Rh(η^1-CO_2)(Cl)(diars)$_2$. *J. Am. Chem. Soc.* **1983**, *105* (18), 5914-5915.

(4) Jeoung, J.-H.; Dobbek, H. Carbon Dioxide Activation at the Ni,Fe-Cluster of Anaerobic Carbon Monoxide Dehydrogenase. *Science* **2007**, *318* (5855), 1461-1464.

(5) Costentin, C.; Drouet, S.; Robert, M.; Savéant, J.-M. A Local Proton Source Enhances CO_2 Electroreduction to CO by a Molecular Fe Catalyst. *Science* **2012**, *338* (6103), 90-94.

(6) Beley, M.; Collin, J. P.; Ruppert, R.; Sauvage, J. P. Electrocatalytic Reduction of Carbon Dioxide by Nickel cyclam^{2+} in Water: Study of the Factors Affecting the

Efficiency and the Selectivity of the Process. *J. Am. Chem. Soc.* **1986**, *108* (24), 7461-7467.

(7) Machan, C. W.; Yin, J.; Chabolla, S. A.; Gilson, M. K.; Kubiak, C. P. Improving the Efficiency and Activity of Electrocatalysts for the Reduction of CO_2 through Supramolecular Assembly with Amino Acid-Modified Ligands. *J. Am. Chem. Soc.* **2016,** *138* (26), 8184-8193.

(8) Machan, C. W.; Chabolla, S. A.; Yin, J.; Gilson, M. K.; Tezcan, F. A.; Kubiak, C. P. Supramolecular Assembly Promotes the Electrocatalytic Reduction of Carbon Dioxide by Re(I) Bipyridine Catalysts at a Lower Overpotential. *J. Am. Chem. Soc.* **2014**, *136* (41), 14598-14607.

(9) Huckaba, A. J.; Sharpe, E. A.; Delcamp, J. H. Photocatalytic Reduction of CO_2 with Re-Pyridyl-NHCs. *Inorg. Chem.* **2016**, *55* (2), 682-690.

(10) Záliš, S.; Consani, C.; Nahhas, A. E.; Cannizzo, A.; Chergui, M.; Hartl, F.; Vlček Jr., A. Origin of Electronic Absorption Spectra of MLCT-Excited and One-Electron Reduced 2,2′-Bipyridine and 1,10-Phenanthroline Complexes. *Inorganica Chim. Acta* **2011**, *374* (1), 578-585.

(11) Hernández, D. J.; Vázquez-Lima, H.; Guadarrama, P.; Martínez-Otero, D.; Castillo, I. Solution and Solid-State Conformations of 1,5-Pyridine and 1,5-Phenanthroline-Bridged P-Tert-butylcalix[8]arene Derivatives. *Tetrahedron Lett.* **2013**, *54* (36), 4930-4933.

(12) de Bruin, B.; Bill, E.; Bothe, E.; Weyhermüller, T.; Wieghardt, K. Molecular and Electronic Structures of Bis(pyridine-2,6-Diimine)metal Complexes $[ML_2](PF_6)n$ (n = 0, 1, 2, 3; M = Mn, Fe, Co, Ni, Cu, Zn). *Inorg. Chem.* **2000**, *39* (13), 2936-2947.

(13) Arana, C.; Yan, S.; Keshavarz-K., M.; Potts, K. T.; Abruna, H. D. Electrocatalytic Reduction of Carbon Dioxide with Iron, Cobalt, and Nickel Complexes of Terdentate Ligands. *Inorg. Chem.* **1992**, *31* (17), 3680-3682.

(14) Chiericato Jr., G.; Arana, C. R.; Casado, C.; Cuadrado, I.; Abruña, H. D. Electrocatalytic Reduction of Carbon Dioxide Mediated by Transition Metal Complexes with Terdentate Ligands Derived from Diacetylpyridine. *Inorganica Chim. Acta* **2000**, *300-302*, 32-42.

(15) Silveira, V. C.; Abbott, M. P.; Cavicchioli, M.; Gonçalves, M. B.; Petrilli, H. M.; Rezende, L. de; Amaral, A. T.; Fonseca, D. E. P.; Caramori, G. F.; Ferreira, A. M. da C. Peculiar Reactivity of a Di-Imine copper(II) Complex Regarding Its Binding to Albumin Protein. *Dalton Trans.* **2013**, *42* (18), 6386-6396.

(16) Casella, L.; Silver, M. E.; Ibers, J. A. Synthesis and Characterization of copper(I), copper(II), zinc(II), cobalt(II), and iron(II) Complexes of a Chelating Ligand Derived from 2,6-Diacetylpyridine and L-Histidine. Oxygenation of the copper(I), cobalt(II), and iron(II) Complexes. Crystal Structure of the zinc(II) Complex. *Inorg. Chem.* **1984**, *23* (10), 1409-1418.

(17) Casella, L.; Gullotti, M. Coordination Modes of Histidine. 2. Stereochemistry of the Reaction between Histidine Derivatives and Pyridoxal Analogs Conformational

Properties of zinc(II) Complexes of Histidine Schiff Bases. *J. Am. Chem. Soc.* **1981**, *103* (21), 6338-6347.

(18) Sunamoto, J.; Kondo, H.; Kikuchi, J.; Yoshinaga, H.; Takei, S. Intramolecular Cyclization of the Pyridoxal-Histidine Schiff Base Controlled in Reversed Micelles. *J. Org. Chem.* **1983**, *48* (14), 2423-2424.

(19) Goodwin, J. A.; Bodager, G. A.; Wilson, L. J.; Stanbury, D. M.; Scheidt, W. R. The Pentacoordinate [CuI((imidH)$_2$DAP)]+ Cation: Its Structural Verification, Ligand Rearrangement, and Deceptive Reaction with Dioxygen. *Inorg. Chem.* **1989**, *28* (1), 35-42.

(20) Goodwin, J. A.; Stanbury, D. M.; Wilson, L. J.; Eigenbrot, C. W.; Scheidt, W. R. Molecular Structures and Electron-Transfer Kinetics for Some Pentacoordinate Cu(I)/Cu(II) Redox-Active Pairs. *J. Am. Chem. Soc.* **1987**, *109* (10), 2979-2991.

(21) Mathews, I. I.; Manohar, H. Synthesis, Spectral and Structural Studies on Metal Complexes of Schiff Bases Involving Vitamin B_6 and Histamine. *J. Chem. Soc., Dalton Trans.* **1991**, No. 9, 2289-2294.

(22) Coggin, D. K.; Gonzalez, J. A.; Kook, A. M.; Stanbury, D. M.; Wilson, L. J. Ligand Dynamics in Pentacoordinate copper(I) and zinc(II) Complexes. *Inorg. Chem.* **1991**, *30* (5), 1115-1125.